

Magnetic properties of BiMnO₃ nanoparticles in SBA-15 mesoporous silica

This content has been downloaded from IOPscience. Please scroll down to see the full text.

2009 J. Phys.: Conf. Ser. 150 042198

(<http://iopscience.iop.org/1742-6596/150/4/042198>)

View [the table of contents for this issue](#), or go to the [journal homepage](#) for more

Download details:

IP Address: 150.69.123.200

This content was downloaded on 13/03/2017 at 02:48

Please note that [terms and conditions apply](#).

You may also be interested in:

[Synthesis of novel magnetic iron metal–silica \(Fe–SBA-15\) and magnetite–silica\(Fe₃O₄–SBA-15\) nanocomposites with a high iron content using temperature-programed reduction](#)

H H P Yiu, M A Keane, Z A D Lethbridge et al.

[Effect of uniaxial strain on the structural, electronic and elastic properties of orthorhombic BiMnO₃](#)

Pei Yang and Wu Haibin

[A triple-layer design for polyethyleneimine-coated, nanostructured magnetic particles and their use in DNA binding and transfection](#)

H H P Yiu, S C McBain, A J El Haj et al.

[N-heptane adsorption and desorption in mesoporous materials](#)

R Zaleski, M Gorgol, A Bazewicz et al.

[Thermal conductivity of a kind of mesoporous silica SBA-15](#)

Huang Cong-Liang, Feng Yan-Hui, Zhang Xin-Xin et al.

[Production of silver-silica core-shell nanocomposites using ultra-short pulsed laser ablation in nanoporous aqueous silica colloidal solutions](#)

A Santagata, A Guarnaccio, D Pietrangeli et al.

[Large magnetodielectric effect in composites of Fe₂O₃·SiO₂ nanoglass and mesoporous silica](#)

Soumi Chatterjee, Ramaprasad Maiti, Shyamal Kumar Saha et al.

Magnetic properties of BiMnO₃ nanoparticles in SBA-15 mesoporous silica

T Tajiri¹, M Harazono², T Kitamura², H Deguchi², S Kohiki², M Mito², A Kohno¹ and S Takagi²

¹Faculty of Science, Fukuoka University, Fukuoka 814-0180, Japan

²Faculty of Engineering, Kyushu Institute of Technology, Kitakyushu 804-8550, Japan

E-mail: tajiri@fukuoka-u.ac.jp

Abstract. Nanoparticles of multiferroic material BiMnO₃ were synthesized in the pores of the mesoporous silica SBA-15 and their magnetic properties were investigated. The powder X-ray diffraction pattern for the nanoparticles at room temperature was similar to that for bulk crystals with monoclinic symmetry. The particle size of the nanocrystals was estimated to be about 14 nm using Scherrer's equation. The temperature dependence of the DC susceptibilities for the nanoparticles showed superparamagnetic behavior. The susceptibility and thermoremanent magnetization exhibited the ferromagnetic feature and the ferromagnetic transition temperature was almost same to that for bulk crystals, ≈ 100 K. However, the Weiss temperature Θ was evaluated as the negative value and the magnetization curve showed antiferromagnetic behavior. The results suggest the antiferromagnetic properties appeared prominently in the nanoparticles.

1. Introduction

Highly distorted perovskite bismuth manganite BiMnO₃ has been extensively studied as multiferroic material. The ferromagnetic and ferroelectric transition temperatures are $T_M \approx 100$ K and $T_E \approx 750$ K, respectively.[1] A fairly large negative magnetocapacitance effect was observed in the vicinity of the ferromagnetic transition temperature T_M . At T_E , a centrosymmetric-to-non-centrosymmetric structural transition takes place, which describes of the ferroelectricity in the system. The changes in the dielectric constant are induced by the magnetic ordering as well as by the application of magnetic fields near T_M . These features are attributed to the inherent coupling between the ferroelectric and ferromagnetic ordering in the multiferroic system. The electronic configuration of Mn³⁺ ion in BiMnO₃ is $t_{2g}^3 e_g^1$ as a A-type antiferromagnetic compound LaMnO₃, but BiMnO₃ shows ferromagnetic behavior due to the complex orbital ordering.[2] There is no crystallographic phase transition on cooling the polar room temperature structure down to 20 K, support to the belief that ferromagnetism and ferroelectricity coexist in BiMnO₃.

The magnetic nanoparticles generally show many interesting behaviors and magnetic size effects such as superparamagnetism, decrease in the transition temperature and quantum tunneling. It is interesting to investigate the magnetic size effects on the BiMnO₃ nanoparticles because the BiMnO₃ bulk crystals show unique magnetic properties. We synthesized the BiMnO₃ nanoparticles in the pores of mesoporous silica SBA-15 and investigated their magnetic properties.

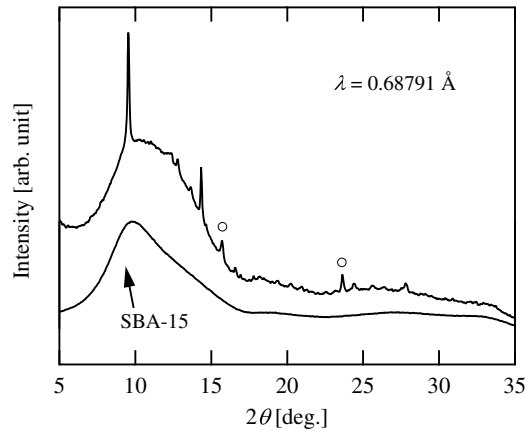


Figure 1. Powder X-ray diffraction patterns for BiMnO₃ nanoparticles and for SBA-15 at room temperature. The circle symbols show diffraction peaks of impurity phase BiOCl or Bi₂O₂CO₃.

2. Experimental

The BiMnO₃ nanoparticles were synthesized in the pores of the mesoporous silica SBA-15 with a diameter of about 8 nm. The SBA-15 has well ordered two-dimensional hexagonal mesoporous silica structure.[3, 4] The BiMnO₃ nanoparticles were synthesized by soaking the molecular sieves in stoichiometric aqueous solution of BiCl₃ and Mn(CH₃COO)₂·4H₂O. Then, the soaked samples were dried and calcinated in flowing oxygen at 780 °C for 18 hours.

The magnetic properties of BiMnO₃ nanoparticles were measured using a SQUID magnetometer (Quantum Design MPMS-5S). The powder X-ray diffraction measurements at room temperature were carried out using a synchrotron radiation X-ray diffractometer at BL-1B of the Photon Factory (PF) at the Institute of Materials Structure Science, High Energy Accelerator Research Organization (KEK), Japan. The incident X-ray wavelength was 0.68791(3) Å calibrated with the CeO₂ powder diffraction pattern. ESR measurement at room temperature was performed using an X-band spectrometer (JES-RE2X) at about 9.3 GHz.

3. Results and Discussion

Figure 1 shows the powder X-ray diffraction patterns for BiMnO₃ nanoparticles and for SBA-15 at room temperature. The broad background peak at around 2 Θ = 10° in the powder patterns for nanoparticles and SBA-15 originated from the glass capillary. The diffraction pattern for nanoparticles shows some Bragg peaks which correspond to bulk BiMnO₃ with monoclinic symmetry (space group; *C*2) [5] and impurity phase of BiOCl or Bi₂O₂CO₃ shown by circle symbols in Fig. 1. Both impurity phases are nonmagnetic. The particle size of synthesized BiMnO₃ nanoparticles was estimated to be about 14 nm based on the Bragg peaks and using Scherrer's equation. The estimated particle size is slightly larger than the pore size of prepared SBA-15. It is considered that the nanoparticles grew into rod-like structure in the one dimensional pores of the SBA-15. ESR measurement results indicate that there is no impurity of isolated Mn²⁺ ions derived from remaining reagent Mn(CH₃COO)₂·4H₂O without synthesis reaction. The X-ray diffraction and ESR measurement results suggest that there are not any magnetic impurities in the prepared samples.

Figure 2 shows the temperature dependence of DC susceptibilities and inverse susceptibilities for BiMnO₃ nanoparticles. The susceptibilities were measured under an external field $H = 100$ Oe in both the field-cooled (FC) and zero-field-cooled (ZFC) conditions. A pronounced irreversibility between FC and ZFC susceptibilities was observed. The bulk crystal also showed a

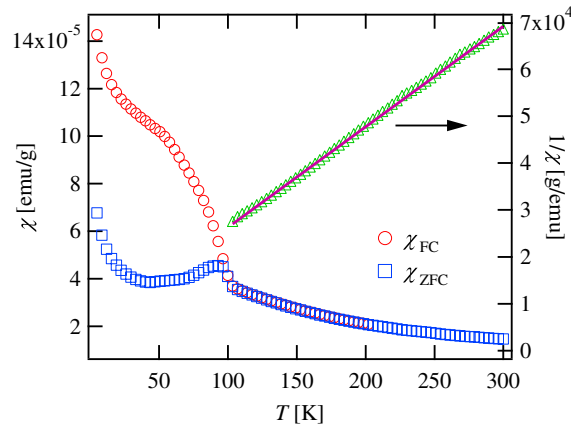


Figure 2. Temperature dependence of DC susceptibilities at field of $H = 100$ Oe in the field-cooled condition (circle symbols) and zero-field-cooled condition (square symbols). Right axis gives the inverse susceptibilities (triangle symbols) with the Curie-Weiss fit (line).

irreversibility of susceptibility below ferromagnetic transition temperature due to the appearance of a spin glass like state. [6] In the present results for nanoparticles, the irreversibility was attributed to the blocking phenomena due to the superparamagnetism because the nonlinear susceptibility did not show a critical divergence as observed for spin glass state. In addition, the behavior of nonlinear susceptibility suggested that there was no pronounced interparticle dipole interaction. The susceptibilities showed the ferromagnetic ordering at 98 K which was similar to the ferromagnetic transition temperature for bulk crystal. The thermoremanent magnetization curve was measured at zero magnetic field on heating after cooling the sample at $H = 1000$ Oe. The thermoremanent magnetization decreased toward zero with increasing temperature and became constant value above the transition temperature. The behavior suggests a ferromagnetic relaxation process. However, the inverse susceptibilities between 100 K and 300 K were fitted by the Curie-Weiss equation with a negative Weiss temperature, $\Theta = -34$ K, as shown by a fitting line in Fig. 2. The estimated value of Θ for nanoparticles presents remarkable difference with $\Theta = 126.1$ K for bulk crystals [6] in the sense of both the sign and magnitude.

Figure 3 shows the magnetization curves at $T = 5$ K, 50 K and 70 K. Though the magnetic susceptibilities showed the ferromagnetic ordering, the magnetization curves below the ordering temperature exhibited linearly increase without rapidly increase under a low field. The magnetization curves for nanoparticles were quite different from that for bulk crystals and seemed to be the antiferromagnetic behavior rather than ferromagnetic one. The magnetization curves below the blocking temperature showed a small hysteresis loop due to the blocking phenomena.

The magnetic measurement results for BiMnO_3 nanoparticles showed both ferromagnetic and antiferromagnetic behaviors. The coexistence of a ferromagnetic component and an antiferromagnetic one was observed in LaMnO_3 and hole doped $\text{La}_{1-x}\text{Sr}_x\text{MnO}_3$ nanocrystals with a diameter of about 8 nm, which was attributed to complex phase diagram of bulk crystals depended on the hole concentration and phase separation. [7, 8] Neutron diffraction investigation for BiMnO_3 bulk crystals indicated that BiMnO_3 has six unique Mn-O-Mn superexchange pathway between the three crystallographically independent Mn^{3+} sites which consist of four ferromagnetic interactions and two antiferromagnetic interactions. The ferromagnetism of BiMnO_3 stems directly from orbital ordering related to a strong distortion of MnO_6 octahedra due to Jahn-Teller distortion. [2, 5, 9] The present results for nanoparticles indicated obvious

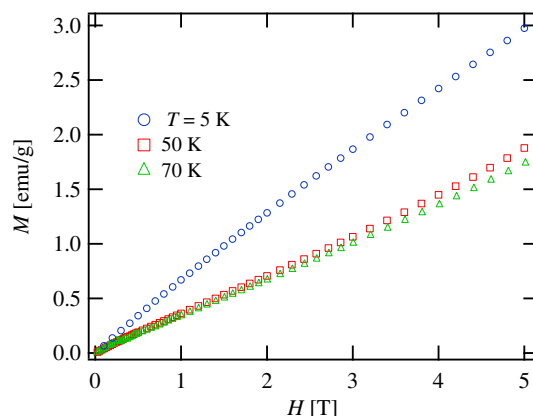


Figure 3. Magnetization curves for BiMnO₃ nanoparticles at $T = 5$ K, 50 K and 70 K.

existence of antiferromagnetic component. It is considered that the change of the orbital ordering pattern or orbital melting is induced in the nanoparticles, and consequently the antiferromagnetic behavior appears. The unique magnetic size effects of BiMnO₃ nanoparticles are derived from the complicated properties of bulk crystals in a similar manner to those of La_{1-x}Sr_xMnO₃ nanocrystals.

In summary, we synthesized BiMnO₃ nanoparticles with a diameter of about 14 nm in the pores of mesoporous silica SBA-15 and investigated their magnetic properties. The temperature dependence of magnetic susceptibilities showed ferromagnetic behavior with ferromagnetic transition temperature similar to that of bulk crystal. The thermoremanent magnetization curve showed a ferromagnetic relaxation process. However, the Weiss temperature for nanoparticles was evaluated as a negative value and the magnetization curves showed antiferromagnetic behavior. The magnetic measurement results for bulk crystal consistently showed ferromagnetic behavior, but those for nanoparticles exhibited both ferromagnetic and antiferromagnetic properties. The present results suggest that the appearance of antiferromagnetic properties is characteristic of the present nanoparticles.

Acknowledgments

The SQUID and ESR measurements were carried out at the Center for Instrumental Analysis, Kyushu Institute of Technology. The X-ray diffraction measurements using a synchrotron-radiation X-ray diffractometer were performed at the Photon Factory, KEK. This work was supported by Grand-in-Aid Scientific Research on Priority Areas (19052006).

References

- [1] Kimura T, Kawamoto S, Yamada I, Azuma M, Takano M and Tokura Y 2003 *Phys. Rev. B* **67** 180401(R).
- [2] Moreira dos Santos A, Cheetham A K, Atou T, Syono Y, Yamaguchi Y, Ohoyama K, Chiba H and Rao C N R 2002 *Phys. Rev. B* **66** 064425.
- [3] Zhao D, Feng J, Huo Q, Melosh N, Fredrickson G H, Chmelka B F and Stucky G D 1998 *Science* **279** 548.
- [4] Kruk M, Jaroniec M, Ko C H and Ryoo R 2000 *Chem. Mater.* **12** 1961.
- [5] Atou T, Chiba H, Ohoyama K, Yamaguchi Y and Syono Y 1999 *J. Solid State Chem.* **145** 639.
- [6] Belik A A and Takayama-Muromachi E 2006 *Inorg. Chem.* **45** 10224.
- [7] Tajiri T, Deguchi H, Kohiki S, Mito M, Takagi S, Tsuda K and Murakami Y 2006 *J. Phys. Soc. Jpn.* **75** 113704.
- [8] Tajiri T, Deguchi H, Kohiki S, Mito M, Takagi S, Mitome M, Murakami Y and Kohno A (to be published).
- [9] Belik A A, Iikubo S, Yokosawa T, Kodama K, Igawa N, Shamoto S, Azuma M, Takano M, Kimoto K, Matsui Y and Takayama-Muromachi E 2007 *J. Am. Chem. Soc.* **129** 971.